Multiple Working Mode Control of Door-Opening With a Mobile Modular and Reconfigurable Robot

Saleh Ahmad, Hongwei Zhang, and Guangjun Liu, *Senior Member, IEEE*

***Abstract*—This paper addresses the problems of opening a door with a modular and reconfigurable robot (MRR) mounted on a wheeled mobile robot platform. The main concern of opening a door is how to prevent the occurrence of large internal forces that arise because of the positioning errors or imprecise modeling of the robot or its environment, specifically, the door parameters. Unlike previous methods that relied on compliance control, making the control design rather complicated, this paper presents a new concept that utilizes the multiple working modes of the MRR modules. The control design is significantly simplified by switching selected joints of the MRR to work in passive mode during door-opening operation. As a result, the occurrence of large internal forces is prevented. Different control schemes are used for control of the joint modules in different working modes. For the passive joint modules, a feedforward torque control approach is used to compensate the joint friction to ensure passive motion. For the active joint modules, a distributed control method based on torque sensing is used to facilitate the control of joint modules working under this mode. To enable autonomous door-opening, an online door parameter estimation algorithm is proposed on the basis of the least squares method, and a path planning algorithm is developed on the basis of Hermite cubic spline functions, with consideration of motion constraints of the mobile MRR. Simulation and experimental results are presented to show the effectiveness of the proposed approach.**

***Index Terms*—Door-opening, mobile manipulation, motion and path planning, multiple working mode control.**

I. Introduction

MODERN robot applications, including mobile manipulation, have far higher performance demands than those of assembly and repetitive tasks. Mobile manipulators become more useful when they perform tasks that are second nature to humans, such as door-opening. Humans can readily tell a door's-opening direction and then apply appropriate force to open the door. In doing so, they instinctively use vision, memory, and/or trial-and-error to quickly estimate the radius of the door and the position of the hinge. The human brain processes the gathered information to help determine the correct direction of the force application. Performing the same tasks with mobile robot manipulators is quite challenging and usually requires sophisticated control and/or mechanical designs in order to perform them adequately.

One of the fundamental requirements for successfully opening a door with a mobile manipulator is the proper handling of the interaction between the manipulator and the door. The interaction forces sensed at the robot's end-effector are of concern. Because of the inevitable positioning errors of the mobile base, large internal forces can be generated. Excessive internal forces are undesirable, as they may cause the task to fail or may even cause damage to the hardware.

Conventional robot manipulators use position control and need specific programming that is tailored to precise requirements of a task, with poor adaptability to changes in the environment and great sensitivity to modeling errors. In addition, precise path or trajectory planning for robot manipulators requires accurate kinematics modeling, which is not always possible for a mobile manipulator. Introduction of force-feedback control in robot manipulators gives advantages of versatility and adaptability but has its own problems when implemented in real time. Since force sensors detect external forces by amplifying the strain of strain gauges, signal noise is also amplified. High-frequency noise can be reduced by using low-pass filters; however, the frequency band of force sensing becomes very narrow [1]. Filtering the force signal also adds an unacceptable lag. Therefore, stability problems and severe performance degradation may result.

To handle the problem of excessive internal forces, the existing literature has focused on the use of compliance control and multitactile sensors. Some researchers chose to explore new designs of compliant mechanisms that lead to a robotic system dedicated to a door-opening task [2], [3]. For the door-opening task, active working mode is required for the manipulator to approach and grasp the door knob. During the door-opening process, some form of passivity is desirable to prevent the occurrence of large internal forces.

In this paper, we focus on pulling a door knob to open a door. Unlike existing methods, this paper presents a new approach to the door-opening problem in the sense that it does not require complicated compliance control design or any special mechanical design of the robot end-effector. The proposed approach relies on the multiple working modes of the modular and reconfigurable robot (MRR) joints to prevent the occurrence of large internal forces by choosing some joints to work in passive mode. After grasping and rotating the door knob by the MRR robot, multiple working mode control is used to slightly open the door by only moving the MRR robot. While in this process, the initial position of the mobile base and the door parameters

Manuscript received June 17, 2011; revised November 27, 2011; accepted February 4, 2012. Recommended by Technical Editor G. Yang. This work was supported in part by a research grant from the Natural Sciences and Engineering Research Council of Canada and in part by the Canada Research Chair program.

The authors are with the Department of Aerospace Engineering, Ryerson University, Toronto, ON M5B 2K3, Canada (e-mail: saleh1.ahmad@ryerson.ca; hongwei.zhang@ryerson.ca; gjliu@ryerson.ca).

Color versions of one or more of the figures in this paper are available online at http://ieeexplore.ieee.org.

Digital Object Identifier 10.1109/TMECH.2012.2191301

are estimated using the proposed parameter estimation method. These estimated parameters are then used for planning a safe path of the mobile base. Finally, the mobile base starts following the desired path, while the MRR robot is working under multiple working mode control to prevent the occurrence of large internal forces.

II. Related Work

Research works have been reported in the literature of door-opening control using a mobile robot manipulator, mostly based on a combination of position and force control. Nagatani and Yuta [4]–[6] presented a strategy for opening doors that makes use of an analytical description of the door handle trajectory. In their research, with the assumption of the position and radius of the door known, they applied the concept of action primitives to door-opening. Each action primitive is equipped with an error adjustment mechanism to cope with accumulated positioning errors of the mobile base. Niemeyer and Slotine [7] proposed a control method of following the path of least resistance to solve the problem of door-opening, which does not require a kinematic model of the door but needs high-resolution joint velocity measurement. Petersson *et al*. [8] proposed a high-level control approach that uses off-the-shelf algorithms for force/torque control for door-opening tasks using mobile manipulators. Their results demonstrate that the control design using hybrid dynamic system models can reduce error magnitudes considerably during the door handle grasping task. Kragic *et al*. [9] demonstrated an intelligent control architecture for finding the doorknob by visual servoing and then estimating the door parameters. In their proposed method, they integrated vision and control system where the objective is to provide information required to switch between control modes of different complexity. Waarsing *et al*. [10] proposed a behavior-based controller for door-opening with a mobile manipulator. The key for realizing such a behavior-based controller is the cooperation among the mobile manipulator subsystems, i.e., the locomotion and the manipulator control system. Chung *et al*. [11] designed a multifingered robotic hand for an indoor service robot PSR1. Active sensing algorithms are proposed to reduce the effect of uncertainties in the environment. Fingertip tactile sensors are used for estimating the contact force and the contact position. The computed contact force is used to carry out compliance control of the door-opening process. Kim *et al*. [12] developed a special mobile manipulator called Hombot for opening a door. Hombot is equipped with an anthropomorphous arm with a double active universal joint (DAUJ) to guarantee a compact size of the manipulator. Compliant control is used for the relaxation of the end-effector to successfully accomplish the door-opening task. Brooks *et al*. [13] developed a mobile robot manipulator system called CARDEA to push open doors. It relies on behavior and sensorimotor control where behaviors of the robot here refer to actions like *following a corridor* or *approaching a door*. CARDEA uses a SEGWAY base mechanism for locomotion equipped with a 15-DOF robotic arm. The robotic arm is designed for an unstructured environment and comprises a series of elastic actuators to analyze the response of behavior-based methods and dexterous manipulation. Through virtual spring models, human-like response was obtained and the results were experimentally verified. However, this robot is capable of opening ajar doors only, as it is not designed for grasping and turning the door handle or knob. Klingbeil *et al*. [14] developed a vision-based learning algorithm capable of opening various types of doors without prior knowledge of the door parameters. Kobayashi *et al*. [2] have been developing a series of rescue robots named UMRS (Utility Mobile Robots for Search) since the Great Hanshin–Awaji earthquake in 1995. In their recent version, they implemented a door-opening system using compliant mechanisms.

To the best of our knowledge, the reported works are all based on mobile manipulators equipped with conventional robotic arms working only in active mode. As a result, compliance control approaches involving force/position control algorithms are demanded to reduce the effects of the internal forces at the end-effector resulting from the interaction with the door. We have developed an MRR with joint modules supporting multiple working modes, specifically active and passive working mode [15]. By carefully choosing when and which joint module should be switched between these two working modes, the problem of door-opening is addressed in this paper without the need for compliance control and with less sensory and computational complexity.

III. Problem Formulation

The focus of this paper is on the door-opening and we assume that the reaching/grasping task has been accomplished. The robot end-effector is constrained to move along the circular trajectory of the door knob throughout the door-opening task. When using conventional robots with joints capable of working only in active mode, the occurrence of large internal forces is inevitable due to the positioning and modeling errors. Compliant control algorithms are, therefore, a requirement for door-opening tasks, but they come at complexity and computational cost. A planar model of the door-opening process is depicted in Fig. 1. The door knob motion is assumed to follow an arc trajectory in the xy plane with a center of rotation at (x_0, y_0) and a radius r. With the assumption that the gripper holds the door knob firmly, the knob's position forms the gripper's trajectory during door-opening process. The following relation has to hold at all times:

$$r^2 = (x - x_0)^2 + (y - y_0)^2.$$

With the robot supporting only active working mode, the methods for control during the described door-opening task may be summarized as follows. Assuming that the absolute path of the door knob is accurately known, one approach is to command the robot to follow the door knob path using a standard position or trajectory controller. This is perhaps the most impractical approach as a small positioning error of the mobile manipulator may create large internal forces. Another approach is to include the door mechanism into the full dynamic model of the manipulator as an overactuated closed kinematic chain [16], then use the extra motors to control the internal forces. While

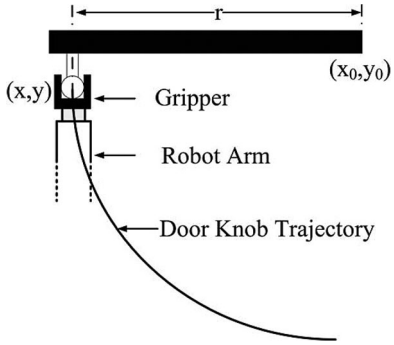

Fig. 1. Planar model of door-opening.

theoretically justifiable, this again is intolerant of kinematic modeling errors. To deal with the problem of large internal forces, complicated control techniques such as compliant motion control or predictive control are studied to relax the internal forces [17]. These control techniques are based on force-feedback control and usually have a slow response and a high computational cost.

We propose a new approach to the door-opening problem based on the framework of multiple working mode control proposed in [15] and [18]. The multiple working mode control is used to prevent the occurrence of large internal forces by switching between active and passive working modes.

IV. Description of the Mobile MRR Robot

A. MRR Robot

Four MRR modules plus a gripper, providing 5 DOF, have been developed in our laboratory. A picture of the MRR robot is shown in Fig. 2. Each joint module consists of a brushless DC motor, an encoder, a braking system, homing and limit sensors, a harmonic drive with an integrated torque sensor, and an amplifier. A six-axis force sensor is mounted on the MRR wrist module. Multiple working modes are implemented on each joint module; each module can, therefore, independently work in active mode with position or force control, or passive mode with friction compensation. By sending commands to the DSP card embedded, the corresponding joint module can be switched online to work in either the active or the passive mode. The MRR wrist is developed based on the 2-DOF DAUJ mechanism (see [19]). The motion range of each MRR module is: Joint 1: $\pm 180^\circ$, Joints 2 and 3: $\pm 120^\circ$, DAUJ (Wrist): $\pm 30^\circ$ pitch and yaw.

B. Locomotion Base

The locomotion system in Fig. 2 is based on the PowerBot Automated Guided Vehicle from MobileRobots Inc. It has multiple sensors including a SICK laser rangefinder, a Bumblebee2 stereovision camera with a Pan-Tilt, two arrays of sonar sensors, and bumper sensors. The PowerBot is also equipped with a full-sized onboard PC used for the control of the mobile MRR.

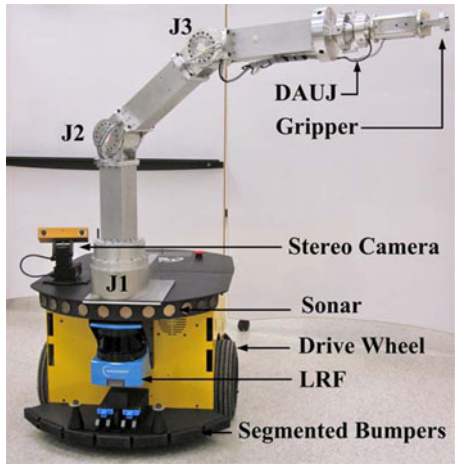

Fig. 2. Five-DOF MRR.

V. Door-Opening

In the proposed door-opening method, after the MRR robot has grasped and rotated the door knob, multiple working mode control is used to slightly open the door using only the MRR robot. During this process, the initial position of the mobile base, the door radius, and the height of the doorknob are estimated using the proposed parameter estimation algorithm. These estimated parameters are then used for planning the path of the mobile base that will allow opening the door to the desired angle. Finally, the multiple working mode control approach is used to control the MRR to complete the door-opening process while preventing the occurrence of large internal forces.

The rest of this section is organized as follows. Section V-A describes the proposed door-opening method. Section V-B addresses estimation of the door parameters followed by path planning of the mobile base. In Section V-D, we provide the control laws used in the multiple working mode control scheme.

A. Door-Opening Method

The door-opening method is proposed with the following assumptions: 1) the door axis of rotation is perpendicular to the floor, i.e., the door knob moves in the horizontal xy plane; this assumption is always true unless there is destruction to the architecture due to earthquakes, which is beyond the scope of this paper; 2) the mobile base travels on almost flat ground, which can always be satisfied for a structured indoor environment; and 3) the axis of rotation of the first MRR module (turret) is perpendicular to the ground, which can be guaranteed by the mechanical design. The basic idea of the proposed door-opening method is to utilize the multiple working modes of the MRR joint modules, to allow the door motion to guide the motion of the MRR robot, so as to avoid the generation of large internal forces. That is achieved by setting the axis of rotation of two joint modules parallel to the door hinge, then switching these joints to work in passive mode during the door-opening process. How to set a joint in the passive working mode will be addressed later in Section V-D. For the aforementioned MRR robot, the axis of rotation of the first joint and that of the fourth joint, part

of the DAUJ, are parallel to the door hinge in the nominal case. To make the axis of rotation of the fourth joint parallel to the door hinge, the second and third joints are set to their desired angles, which will be detailed in Section V-B. The 2-DOF motions of the DAUJ are coupled and cannot be set to work in passive mode independently; thus, the fifth joint is also set in passive mode. The passivity of the 2-DOF DAUJ can compensate for any uncertainty in the active joint positions and/or any misalignment of the axes of rotation of the passive joints and that of the door. The passive joints act like free joints that are passively controlled by the coupling forces of the manipulator; thus, their motion during the door-opening process is directed by the motion of the door itself. The proposed door-opening method can prevent the occurrence of internal forces, as the passive joints can absorb the positioning errors of the mobile manipulator while following the trajectory of the door knob. The movement of the mobile base along the planned trajectory generates the needed force for pulling the door open.

The proposed door-opening method is summarized as follows:

1) grasp the door knob;
2) estimate the door parameters and the mobile base initial position as described in the parameter estimation subsection;
3) calculate the desired path of the mobile base using the estimated parameters;
4) switch the first joint J_1 and the DAUJ J_4 and J_5 to work in passive mode;
5) command the second and third joints to their desired angles calculated from the parameter estimation algorithm; and
6) move the robot base along the predefined trajectory to pull the door open.

A comparison between the traditional and the proposed method is shown in Fig. 3. The proposed method utilizes the multiple working modes feature of the MRR joint modules. It does not require computationally heavy force relaxation algorithms. On the same basis, there is no need for tactile sensors at the gripper fingertips or any special mechanical design to perform the door-opening task. In addition, the MRR robot configuration stays almost unchanged, as only the passive joints are moving throughout the door-opening task. This minimizes the power consumption, which is especially important because the robot arm is running on the mobile base batteries.

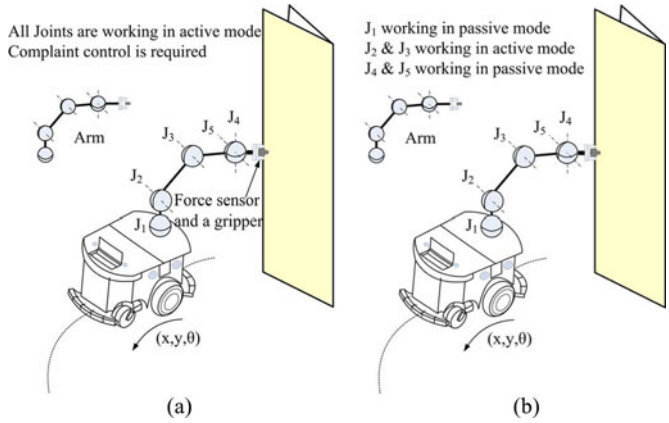

Fig. 3. Comparison between traditional and proposed door-opening method. (a) Traditional method. (b) Proposed method.

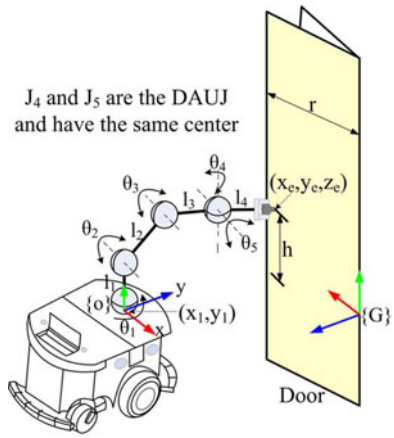

Fig. 4. Initial configuration of the mobile MRR.

B. Parameter Estimation

The mobile base motion during the door-opening process has to be planned such that all joints move within their mechanical limits. In order to plan a safe path for the mobile base, the door parameters as well as the mobile base initial position (x_1, y_1) have to be estimated. The parameters needed to complete the door-opening task are the door radius r and the knob height with respect to the base of the MRR, h. Here, we employ the method of least squares estimation to solve this problem. The idea is to estimate the door parameters and the initial mobile base position by using a recorded motion of the MRR end-effector.

Fig. 4 shows the initial configuration of the mobile MRR, where J_i denotes the ith joint. The origin of the reference frame $\{G\}$ is set at the intersection point of the door hinge and the horizontal plane that crosses the origin of the reference frame of the MRR $\{O\}$. After the MRR end-effector has firmly grasped the door knob, we then, in the estimation process, apply a small torque only to the second joint to slightly open the door. At the same time, all other joints are set in the passive working mode. The MRR end-effector positions are recorded during this process. The saved data are then used to estimate the unknown door parameters as well as the current position of the mobile base. Let (x_e, y_e, z_e) denote the tip position of the end-effector in the reference frame, l_i denote the length of the ith link, θ_i denote the rotation angle of the ith joint, $C_i(t)$, $S_i(t)$, $C_{ij}(t)$, $S_{ij}(t)$ denote $\cos(\theta_i(t))$, $\sin(\theta_i(t))$, $\cos(\theta_i(t) + \theta_j(t))$, $\sin(\theta_i(t) + \theta_j(t))$, respectively. From Fig. 4, with respect to the door radius r, we have

$$x_e^2(t) + y_e^2(t) = r^2 \tag{1}$$

$$z_e(t) = h. \tag{2}$$

With respect to the reference frame $\{G\}$ shown in Fig. 4 and coordinate transfer, we derive

$$x_e(t) = x_1 + l_4C_5(t)(C_1(t)S_4(t) + S_1(t)C_4(t)C_{23}(t)) + l_2S_1(t)C_2(t) + l_3S_1(t)C_{23}(t) - l_4S_1(t)S_5(t)S_{23}(t) \quad (3)$$

$$y_e(t) = y_1 + l_4C_5(t)(S_1(t)S_4(t) - C_1(t)C_4(t)C_{23}(t)) - l_2C_1(t)C_2(t) - l_3C_1(t)C_{23}(t) + l_4C_1(t)S_5(t)S_{23}(t) \quad (4)$$

$$z_e(t) = l_1 + l_4S_5(t)C_{23}(t) + l_4C_4(t)C_5(t)S_{23}(t) + l_2S_2(t) + l_3S_{23}(t). \quad (5)$$

For simplicity, let us introduce the two function definitions $L_x(t)$ and $L_y(t)$, which are functions of explicitly known parameters only

$$L_x(t) \triangleq l_4C_5(t)(C_1(t)S_4(t) + S_1(t)C_4(t)C_{23}(t)) + l_2S_1(t)C_2(t) + l_3S_1(t)C_{23}(t) - l_4S_1(t)S_5(t)S_{23}(t)$$

$$L_y(t) \triangleq l_4C_5(t)(S_1(t)S_4(t) - C_1(t)C_4(t)C_{23}(t)) - l_2C_1(t)C_2(t) - l_3C_1(t)C_{23}(t) + l_4C_1(t)S_5(t)S_{23}(t).$$

Substituting $L_x(t)$ and $L_y(t)$ into (3) and (4) and the resultant equations into (1) and rearranging each term, we have

$$L_x^2(t) + L_y^2(t) = r^2 - x_1^2 - y_1^2 - 2x_1L_x(t) - 2y_1L_y(t). \quad (6)$$

Let us define

$$P = \begin{bmatrix} 1 & 2L_x(t_1) & 2L_y(t_1) \\ \vdots & \vdots & \vdots \\ 1 & 2L_x(t_n) & 2L_y(t_n) \end{bmatrix}, \quad W = \begin{bmatrix} L_x^2(t_1) + L_y^2(t_1) \\ \vdots \\ L_x^2(t_n) + L_y^2(t_n) \end{bmatrix}$$

$$\lambda = \begin{bmatrix} r^2 - x_1^2 - y_1^2 \\ -x_1 \\ -y_1 \end{bmatrix}.$$

Equation (6) can be rewritten as

$$W = P\lambda. \quad (7)$$

A straightforward least-squares approximation is then performed

$$\hat{\lambda} = (P^TP)^{-1}P^TW \quad (8)$$

where $\hat{\lambda}$ is the least squares estimate for the unknown parameters. The axis of rotation of the MRR fourth joint shown in Fig. 4 needs to be parallel to the door hinge, as was explained in Section V-A. This can be easily done by setting the second and third joint angles to their desired values calculated as follows. Once h is known, the desired rotation angle of the second joint can be calculated from

$$\theta_{2d} = \sin^{-1}\left(\frac{h - l_1}{l_2}\right). \quad (9)$$

The rotation angle of the third joint is calculated from the inverse kinematics of the MRR robot, $\theta_{3d} = -\theta_{2d}$. At that moment, the axis of rotation of the first and fourth joints is parallel to the door hinge. The other estimated parameters including the door radius and the mobile base initial position are used for completing the path planning part.

C. Path Planning

There are constraints that have to be considered when planning the trajectory of the mobile base. These constraints can be categorized into kinematic constraints, mechanical constraints, and geometrical constraints. The kinematic constraints are due to the constrained motion of the robot that leads to a reduced number of degrees of freedom. The mechanical constraints are related to the mechanical structure of the robot, e.g., joint limits, maximum speeds, and maximum applicable torque and force at each joint module. Geometrical constraints exist between the door and the mobile base and collision has to be avoided throughout the door-opening process. The objective of this section is to develop a path planning algorithm for the door-opening task that takes the constraints imposed on the mobile MRR into consideration. The implementation of Hermite cubic splines as a tool for path planning is adopted to achieve this goal. Let $p = p_1, p_2, \ldots, p_n$ denote a set of control points (knots) on a route with each point p_i comprising three basic elements, x_i, y_i, and θ_i, $i = 1, 2, \ldots, n$; x_i, y_i denotes the position relative to a global reference frame; θ_i is the heading angle of the mobile robot. Although there are several methods to join these points with a curve, an effective one is piecewise cubic polynomials, also referred to as cubic splines. These cubic splines are ideal, as they provide continuity in position, heading, curvature, velocity, and acceleration [20], [21]. Considering just the local parameterization of the ith cubic spline segment in only the x direction, we have

$$X_i(t) = a_i(t-1)^2(2t+1) + b_it^2(3-2t) + c_it(t-1)^2 - d_it^2(1-t) \quad (10)$$

where X_i denotes the segment connecting the points p_i and p_{i+1} in the x-direction; $0 \le t \le 1$ denotes the relative motion time of each segment i ($i = 1, 2, \ldots, n-1$ segments); n denotes the total number of control points used on the path, and a_i, b_i, c_i, and d_i are the coefficients to be determined. The Hermite cubic polynomial (10) is selected so that it satisfies all four of the following boundary conditions [21]:

$$X_i(0) = a_i; \quad \frac{dX_i}{dt}(0) = c_i, \quad X_i(1) = b_i, \quad \frac{dX_i}{dt}(1) = d_i. \quad (11)$$

The first two boundary conditions are used to, respectively, assign the initial position and velocity values and the last two boundary conditions are used to assign the final position and velocity values. The following additional constraints must be imposed to ensure continuity between each polynomial:

$$X_i(1) = p_{x_{i+1}}, \quad X_i(1) = X_{i+1}(0)$$
$$\frac{dX_i}{dt}(1) = \frac{dX_{i+1}}{dt}(0), \quad \frac{d^2X_i}{dt^2}(1) = \frac{d^2X_{i+1}}{dt^2}(0). \quad (12)$$

For n control points, there are $4(n-1)$ equations and $4(n-1)$ unknowns. The system of equations (11) and (12) can be rewritten in a simple symmetric tridiagonal system of equations as follows:

$$\begin{bmatrix} 1 & & & & & \\ 1 & 4 & 1 & & & \\ & \ddots & \ddots & \ddots & & \\ & & 1 & 4 & 1 & \\ & & & & 1 & \end{bmatrix} \begin{bmatrix} \eta_0 \\ \eta_1 \\ \vdots \\ \eta_{n-2} \\ \eta_{n-1} \end{bmatrix} = \begin{bmatrix} v_{\text{init}} \\ 3(p_{x_3} - p_{x_1}) \\ \vdots \\ 3(p_{x_{n-1}} - p_{x_{n-3}}) \\ v_{\text{final}} \end{bmatrix} \tag{13}$$

where η is an intermediate variable; v_{init} and v_{final} are the initial and final velocities of the path, respectively. The coefficients of the spline are obtained by solving for the intermediate variables $\eta's$

$$a_i = p_{x_i}, \quad b_i = p_{x_{i+1}}, \quad c_i = \eta_{i-1}, \quad d_i = \eta_i. \tag{14}$$

The initial position of the mobile base in the global reference frame was identified from the unknown parameter estimation algorithm. The final position is calculated based on the desired door-opening angle. First, we introduce an intermediate point between the known start and final positions of the mobile base. Afterward, a Hermite cubic polynomial is used to connect these points to create a rudimentary path. Finally, this created path is validated with respect to the constraint imposed on the system. These constraints and the margin in which the mobile robot can move are studied through computer simulation. For each door-opening angle, the position of the mobile base was varied and an algorithm that checks the joint limits and other constraints was used to verify if that position is valid. The algorithm is described as follows.

1) For the current door-opening angle starting from 0°:
   a) calculate the door knob position;
   b) for the current mobile base position starting from the initial position, solve the inverse kinematics of the MRR considering the joint limits and check if the door knob is in the robot workspace;
   c) if (b) holds, using the mobile base footprint, calculate the distance between the door and the mobile base to verify that there is no possible collision;
   d) if (b) and (c) hold, save the mobile base position as a valid position.
2) Change the mobile base position by adding small Δx and Δy.
3) Go to step (1) until one or more of the conditions is no longer satisfied.
4) Increase the door-opening angle and repeat (1) to (3).

Using the aforesaid algorithm, the margin shown in Fig. 5 was obtained. Mobile base motion inside this margin will not violate any of the constraints and hence is allowed. We select the desired path to be in the middle of this margin to guarantee that all constraints are satisfied even in the case of large position errors of the mobile base.

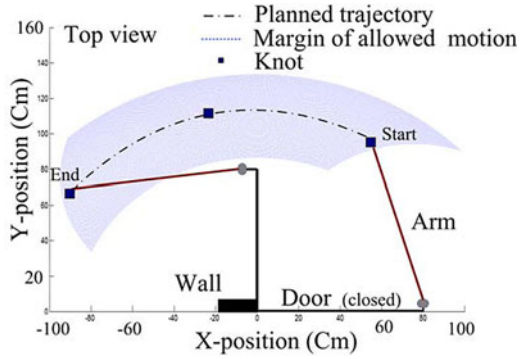

Fig. 5. Trajectory of the mobile base and the margin of allowed motion.

D. Multiple Working Mode Control Design

The working modes of the MRR joint modules are categorized into two types: passive mode and active mode. The passive mode refers to the mode in which a joint rotates freely with friction compensation. The active mode refers to the mode in which a joint module is working under motion or force control.

1) Passive Mode: Friction tends to prevent the output of the joint from moving freely, which has to be compensated to enable the joint working in passive mode. Unlike friction compensation for precise tracking control, passive working mode only needs the joint friction to be compensated such that the joint can be rotated with a small external torque. With the assumption that the frictional memory and rising static friction discussed in [22] are negligible, the friction model can be defined by

$$f_i \triangleq b_i\dot{q}_i + (f_{ci} + f_{si}\exp(-f_{\tau i}\dot{q}_i^2))\text{sgn}(\dot{q}_i) \tag{15}$$

where b_i, f_{ci}, f_{si}, and $f_{\tau i}$ are parameters related to viscous friction, Coulomb friction, static friction, and Stribeck effect, respectively. sgn is a sign function. The compensation method proposed in [15] is not applicable for the scenarios when the desired trajectory of passive joints is unknown. It should be noted that the motion trend of each joint is usually known or predicable in practical applications and the joint angle and angular speeds are normally measurable. The motion direction of each passive joint is also achievable with the torque sensor measurement. On the basis of motion trend and angular speed of the passive joint, a feedforward torque can be applied to compensate the friction and enable joint working in passive mode, as follows:

$$\tau_i = f_{mi}\text{sgn}(\dot{q}_i) + b_i\dot{q}_i, \quad i = 1, \ldots, n \tag{16}$$

where f_{mi} denotes the constant part of the friction, which is less than the static friction f_{si} and its magnitude normally dominates the overall magnitude of the total friction at low speed. With the feed-forward torque shown in (16), the friction can be substantially compensated.

2) Active Mode: With the growing interest in MRRs, more and more efforts are being made in analysis, modeling, and control of MRR robots [23], [24]. For our MRR robot, a distributed control method based on joint torque sensing has been proposed in [25]. This control method is adopted in this paper to control joint modules working under active mode. For completeness, the active mode control scheme will be presented.

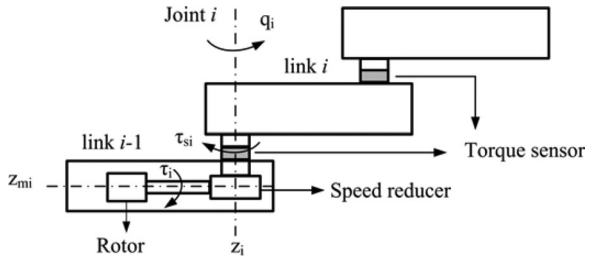

Fig. 6. Schematic diagram of a joint module.

a) Model formulation: Consider an MRR with rotary joint modules installed in series, as illustrated by the schematic diagram shown in Fig. 6.

The following notations are used for the ith module: I_{mi} is the moment of inertia of the ith rotor about the axis of rotation, γ_i is the reduction ratio of the speed reducer ($\gamma_i \geq 1$), q_i is the joint angle, $f_i(q_i, \dot{q}_i)$ is the joint friction, τ_{si} is the coupling torque at the torque sensor location, τ_i is the output torque of the rotor, z_{mi} is a unit vector along the axis of rotation of the ith rotor, and z_i is a unit vector along the axis of rotation of joint i. The dynamic equation of each module is formulated based on the dynamic equations of a rigid robot manipulator with n rotary joints and joint torque sensing derived in [26].

For the first joint module (base joint), $i = 1$

$$I_{m1}\gamma_1\ddot{q}_1 + f_1(q_1, \dot{q}_1) + \frac{\tau_{s1}}{\gamma_1} = \tau_1. \tag{17}$$

For the second joint module from the base, $i = 2$

$$I_{m2}\gamma_2\ddot{q}_2 + f_2(q_2, \dot{q}_2) + I_{m2}z_{m2}^T z_1 \ddot{q}_1 + \frac{\tau_{s2}}{\gamma_2} = \tau_2. \tag{18}$$

For $i \geq 3$

$$I_{mi}\gamma_i\ddot{q}_i + f_i(q_i, \dot{q}_i) + I_{mi}\sum_{j=1}^{i-1} z_{mi}^T z_j \ddot{q}_j + I_{mi}\sum_{j=2}^{i-1}\sum_{k=1}^{j-1} z_{mi}^T(z_k \times z_j)\dot{q}_k\dot{q}_j + \frac{\tau_{si}}{\gamma_i} = \tau_i. \tag{19}$$

The joint friction $f_i(q_i, \dot{q}_i)$ is assumed to be a function of the joint position and velocity as in [27]

$$f_i(q_i, \dot{q}_i) = (f_{ci} + f_{si}\exp(-f_{\tau i}\dot{q}_i^2))\mathrm{sgn}(\dot{q}_i) + b_i\dot{q}_i + f_{qi}(q_i, \dot{q}_i) \tag{20}$$

where b_i, f_{ci}, f_{si}, and $f_{\tau i}$ have the same implications as those in (15), and $f_{qi}(q_i, \dot{q}_i)$ represents the position dependency of friction and other friction modeling errors. The nonparametric friction term $f_{qi}(q_i, \dot{q}_i)$ is bounded as

$$f_{qi}(q_i, \dot{q}_i) < \rho_{fq}^i \tag{21}$$

where ρ_{fq}^i is a known bound.

b) Control design: Let the overall control for each joint be defined by

$$\tau_i = \frac{\tau_{si}}{\gamma_i} + u_i, \quad i = 1, 2, \ldots, n \tag{22}$$

where u_i is the ith joint's new control input to be designed. For the first joint, combining (22) with (17) yields

$$I_{m1}\gamma_1\ddot{q}_1 + f_1(q_1, \dot{q}_1) = u_1. \tag{23}$$

For the second joint, combining (22) with (18) yields

$$I_{m2}\gamma_2\ddot{q}_2 + f_2(q_2, \dot{q}_2) + I_{m2}z_{m2}^T z_1 \ddot{q}_1 = u_2. \tag{24}$$

For $i \geq 3$, substituting (22) with (19) yields

$$I_{mi}\gamma_i\ddot{q}_i + f_i(q_i, \dot{q}_i) + I_{mi}\sum_{j=1}^{i-1} z_{mi}^T z_j \ddot{q}_j + \sum_{j=2}^{i-1}\sum_{k=1}^{j-1} z_{mi}^T(z_k \times z_j)\dot{q}_k\dot{q}_j = u_i. \tag{25}$$

First, the following system errors are defined:

$$e_i \triangleq q_i - q_{id} \tag{26}$$

$$r_i \triangleq \dot{e}_i + \lambda_i e_i \tag{27}$$

$$a_i \triangleq \ddot{q}_{id} - 2\lambda_i\dot{e}_i - \lambda_i^2 e_i \tag{28}$$

where λ_i is a positive constant. The following two properties are worth noting as they are used in the control law design.

Property 1: Since z_{mi} and z_i are unit vectors along the direction of rotation of the ith rotor and joint, the resulting vector products are bounded as

$$|z_{mi}^T z_j| \leq 1 \quad |z_{mi}^T(z_k \times z_j)| \leq 1.$$

Property 2: The velocity and acceleration of a stabilized joint is bounded, i.e., if the ith joint is stabilized

$$|\dot{q}_i| \leq \rho_{vi} \quad |\ddot{q}_i| \leq \rho_{ai}$$

where ρ_{vi} and ρ_{ai} are known constant bounds.

For the active working mode, to compensate the friction of the ith joint, the scheme developed by Liu *et al*. [28] is adopted where $Y(\dot{q}_i)$ and $\tilde{F}^i$ are defined as

$$Y(\dot{q}_i) = \left[\dot{q}_i\ \mathrm{sgn}(\dot{q}_i)\ \ e^{\hat{f}_{\tau i}\dot{q}_i^2}\mathrm{sgn}(\dot{q}_i)\ \ -\hat{f}_{si}\dot{q}_i^2 e^{-\hat{f}_{\tau i}\dot{q}_i^2}\mathrm{sgn}(\dot{q}_i)\right] \tag{29}$$

$$\tilde{F}^i = [\,\hat{bi} - bi \quad \hat{f}_{ci} - f_{ci} \quad \hat{f}_{si} - f_{si} \quad \hat{f}_{\tau i} - f_{\tau i}\,]^T. \tag{30}$$

Similar to [25], the parametric uncertainty $\tilde{F}^i$ is decomposed as

$$\tilde{F}^i = \tilde{F}_c^i + \tilde{F}_v^i \tag{31}$$

where $\tilde{F}_c^i$ is a constant unknown vector, and $\tilde{F}_v^i$ is the variable parametric model uncertainty that is bounded as

$$|\tilde{F}_v^i| < \rho_{fv}^i. \tag{32}$$

It is well known that an adaptive compensator can be designed to compensate for the constant parametric uncertainty $\tilde{F}_c^i$ and a robust compensator can be designed for the variable part $\tilde{F}_v^i$. Applying the decomposition-based control design approach developed in [28] and [29], the following control input is designed

for stabilizing the first joint:

$$u_1 = I_{m1}\gamma_1 a_1 + \hat{b}_1\dot{q}_1 + (\hat{f}_{c1} + \hat{f}_{s1}\exp(\hat{f}_{\tau 1}\dot{q}_1^2))\text{sgn}(\dot{q}_1) + u_u^1 + Y(\dot{q}_1)(u_{pc}^1 + u_{pv}^1) \tag{33}$$

where u_u^1 is designed to compensate for the nonparametric uncertainty $f_{qi}(q,\dot{q})$; u_{pc}^1 is designed to compensate for the constant parametric uncertainty $\tilde{F}_c^i$, and u_{pv}^1 is designed to compensate for the variable parametric uncertainty $\tilde{F}_v^i$. The compensators u_u^i, u_{pv}^i, and u_{pc}^i are defined as in [25]

$$u_u^i = \begin{cases} -\rho_{fq}^i \frac{r_i}{|r_i|}, & |r_i| > \varepsilon_u^i \\ -\rho_{fq}^i \frac{r_i}{|\varepsilon_u^i|}, & |r_i| \le \varepsilon_u^i \end{cases} \tag{34}$$

$$u_{pc}^i = -k_1 \int_0^t Y(\dot{q}_i)^T r_i \, d\tau \tag{35}$$

$$u_{pv}^i = \begin{cases} -\rho_{fv}^i \frac{\zeta^i}{|\zeta^i|}, & |\zeta^i| > \varepsilon_p^i \\ -\rho_{fv}^i \frac{\zeta^i}{|\varepsilon_p^i|}, & |\zeta^i| \le \varepsilon_p^i \end{cases} \tag{36}$$

where $\zeta^i = Y(\dot{q}_i)^T r_i$, and ε_u^i and ε_p^i are positive control parameters.

The coupling term $I_{mi}\sum_{j=1}^{i-1} z_{mi}^T z_j \ddot{q}_j$ in (19) can be rewritten as

$$I_{mi}\sum_{j=1}^{i-1} z_{mi}^T z_j \ddot{q}_j = -\sum_{j=1}^{i-1} \begin{bmatrix} I_{mi}\hat{\theta}_j^i & I_{mi} \end{bmatrix} \begin{bmatrix} \ddot{q}_j \\ \tilde{\theta}_j^i q_j \end{bmatrix} \triangleq -\sum_{j=1}^{i-1} I_j^i D_j^i \tag{37}$$

where $\hat{\theta}_j^i$ denotes the dot product of the unit vectors z_{mi} and z_j, and $\tilde{\theta}_j^i$ is the alignment error, given by the difference in dot products of the nominal and actual direction vectors [25]. Considering the variable parametric uncertainty in the coupling term $I_{mi}\sum_{j=1}^{i-1} z_{mi}^T z_j \ddot{q}_j$, D_j^i in (37) can be decomposed into a constant plus a bounded variable term as

$$D_j^i = D_{jc}^i + D_{jv}^i \tag{38}$$

and the variable term D_{jv}^i is bounded as

$$|D_{jv}^i| \le \rho_{jd}^i. \tag{39}$$

Similar to [25], an adaptive compensator u_{jc}^i is designed for the constant uncertainty term D_{jc}^i and a robust compensator u_{jv}^i for the variable term D_{jv}^i

$$u_{jc}^i = -k_2 \int_0^t {I_j^i}^T r_i d\tau \tag{40}$$

$$u_{jv}^i = \begin{cases} -\rho_{jd}^i \frac{\sigma_j^i}{|\sigma_j^i|}, & |\sigma_j^i| > \varepsilon_d^i \\ -\rho_{jd}^i \frac{\sigma_j^i}{|\varepsilon_d^i|}, & |\sigma_j^i| \le \varepsilon_d^i \end{cases} \tag{41}$$

where $\sigma_j^i = {I_j^i}^T r_i$, and ε_d^i is a positive control parameter. Also, the coupling term $I_{mi}\sum_{j=2}^{i-1}\sum_{k=1}^{j-1} z_{mi}^T(z_k \times z_j)\dot{q}_k\dot{q}_j$ present in the dynamic model of the ith joint (19) can be rewritten as

$$I_{mi}\sum_{j=2}^{i-1}\sum_{k=1}^{j-1} z_{mi}^T(z_k \times z_j)\dot{q}_k\dot{q}_j = -\sum_{j=2}^{i-1}\sum_{k=1}^{j-1} \begin{bmatrix} I_{mi}\hat{\Theta}_{kj}^i & I_{mi} \end{bmatrix} \begin{bmatrix} \dot{q}_k\dot{q}_j \\ \tilde{\Theta}_{kj}^i \dot{q}_k\dot{q}_j \end{bmatrix} \triangleq -\sum_{j=2}^{i-1}\sum_{k=1}^{j-1} J_{kj}^i P_{kj}^i \tag{42}$$

where the term P_{kj}^i can be decomposed as

$$P_{kj}^i = P_{kjc}^i + P_{kjv}^i \tag{43}$$

and the variable term P_{kjv}^i is bounded as

$$|P_{kjv}^i| \le \rho_{kv}\rho_{jv}. \tag{44}$$

Applying decomposition-based control design, an adaptive compensator V_{kjc}^i is designed for the constant uncertainty term P_{kjc}^i and a robust compensator V_{kjv}^i is designed for the variable part P_{kjv}^i as in [25]. The terms V_{kjc}^i and V_{kjv}^i are defined as

$$V_{kjc}^i = -k_3 \int_0^t {J_{kj}^i}^T r_i d\tau \tag{45}$$

$$V_{kjv}^i = \begin{cases} -\rho_{kv}\rho_{jv}\frac{\beta_{kj}^i}{|\beta_{kj}^i|}, & |\beta_{kj}^i| > \varepsilon_v^i \\ -\rho_{kv}\rho_{jv}\frac{\beta_{kj}^i}{|\varepsilon_{pi}^i|}, & |\beta_{kj}^i| \le \varepsilon_v^i \end{cases} \tag{46}$$

where $\beta_{kj}^i = {J_{kj}^i}^T$ and ε_v^i is a positive control parameter. The control law (33) ensures first joint's stability which, in turn, guarantees the boundedness of the tracking errors, and thus, the boundedness of the magnitudes of $\dot{q}_1$ and $\ddot{q}_1$. Since $\ddot{q}_1$ is bounded, a saturation-based robust compensator can be used to compensate for the effects of $\ddot{q}_1$. Therefore, the control input u_2 for the second joint would be given by the control law developed in [29] with an additional term $I_1^2(u_{1c}^2 + u_{1v}^2)$ to compensate for the effects of $\ddot{q}_1$:

$$u_2 = I_{m2}\gamma_2 a_2 + \hat{b}_2\dot{q}_2 + (\hat{f}_{c2} + \hat{f}_{s2}\exp(\hat{f}_{\tau 2}\dot{q}_2^2))\text{sgn}(\dot{q}_2) + u_u^2 + I_1^2(u_{1c}^2 + u_{1v}^2) + Y(\dot{q}_2)(u_{pc}^2 + u_{pv}^2). \tag{47}$$

Similarly, the control input u_i for the ith joint is given by following expression:

$$u_i = I_{mi}\gamma_i a_i + \hat{b}_i\dot{q}_i + (\hat{f}_{ci} + \hat{f}_{si}\exp(\hat{f}_{\tau_i}\dot{q}_i^2))\text{sgn}(\dot{q}_i) + u_u^i + Y(\dot{q}_i)(u_{pc}^i + u_{pv}^i) + \sum_{j=1}^{i-1} I_j^i(u_{jc}^i + u_{jv}^i) + \sum_{j=2}^{i-1}\sum_{k=1}^{j-1} J_{kj}^i(V_{kjc}^i + V_{kjv}^i). \tag{48}$$

The last two terms of (48) are the compensators for the velocities and accelerations of the lower joints. It has been proved in [25] that the tracking error is uniformly bounded under the control law defined by (22), (33), (47), and (48).

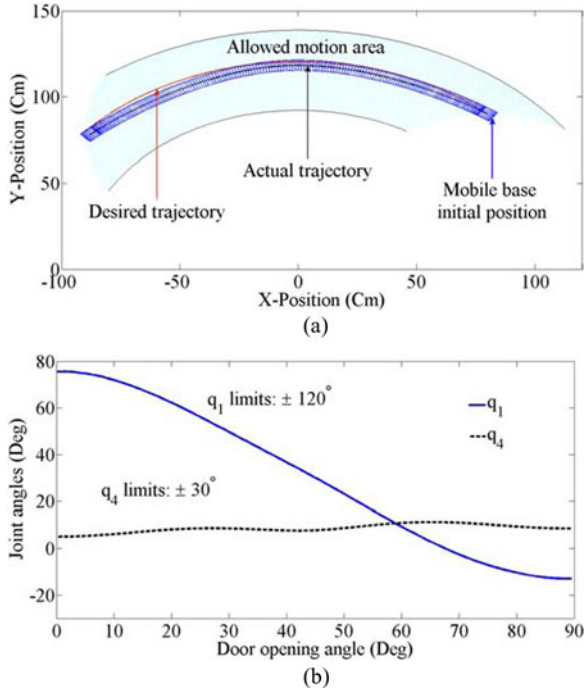

Fig. 7. Simulation results for 2-cm absolute positioning error. (a) Mobile base trajectory with 2-cm positioning error. The light-blue envelope represents the allowed motion area. (b) First and fourth joint angles.

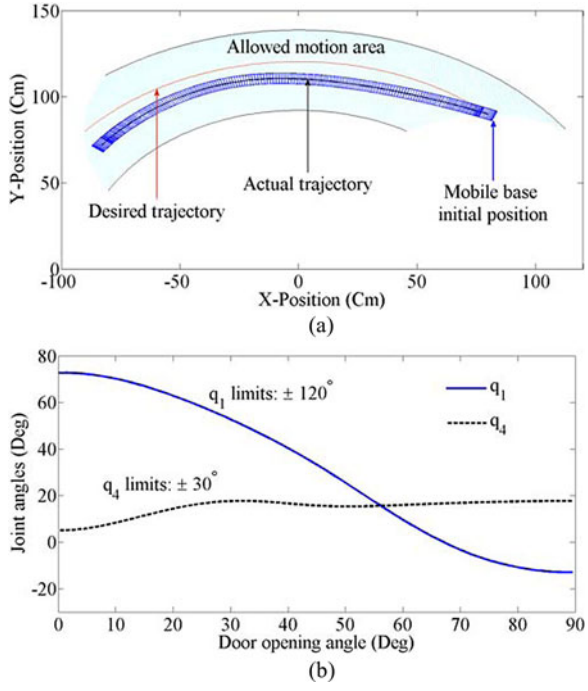

Fig. 8. Simulation results for 10-cm absolute positioning error. (a) Mobile base trajectory with 10-cm positioning error. The light-blue envelope represents the allowed motion area. (b) First and fourth joint angles.

VI. Simulation and Experiment Results

A. Simulation

A series of computer simulations has been carried out to validate the proposed door-opening method and to ensure that all constraints are respected throughout the door-opening process. The mobile base was assumed to have up to 10-cm error in Cartesian space when trying to follow a desired curvature trajectory. This desired trajectory was chosen to be in the middle of the mobile base safe motion margin. The results of some of these simulations are presented in Figs. 7 and 8 with 2- and 10-cm trajectory following errors, respectively. Simulations show that all joints move within their mechanical limits and there is no constraints violation even when the error in Cartesian space is up to 10 cm.

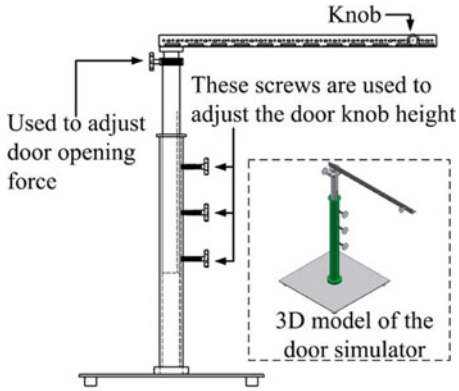

Fig. 9. Schematic diagram of the door simulator.

B. Experiments

At this stage, a door simulator with adjustable radius, knob height, and opening force is used for the door-opening experiment (see Fig. 9). The opening force is adjusted by tightening or releasing a clamp on the door simulator. The knob position and the opening force are selected based on standard door dimensions and opening force. Positioning of the mobile base in front of the door simulator as well as grasping the door knob is done manually. The desired path of the mobile base is calculated by the onboard computer using the estimated door parameters and the mobile base initial position. To this end, several experiments have been performed to confirm the efficiency of the proposed door-opening method, all of which have been successful. The door-opening is shown by sequential pictures in Fig. 10. The joint positions and the readings of the integrated torque sensor of each MRR module as well as the six-axis force sensor were recorded during the door-opening process. Fig. 11 shows the force measurements of the force sensor along the x-, y-, and z-directions. The force in the z-direction Fz represents the pulling force, and it is expected to be large due to the force applied by the door in this direction. The other two forces, Fx and Fy, represent the force in the pitch and yaw directions of the DAUJ, respectively. The torques generated by these forces in the pitch and yaw direction of the DAUJ and the DAUJ joint position angles are shown in Fig. 12. The torque sensor readings of the MRR J_1 and its position angle are shown in Fig. 13. It is clear from the experimental results that the multiple working mode control can prevent the occurrence of large internal forces during

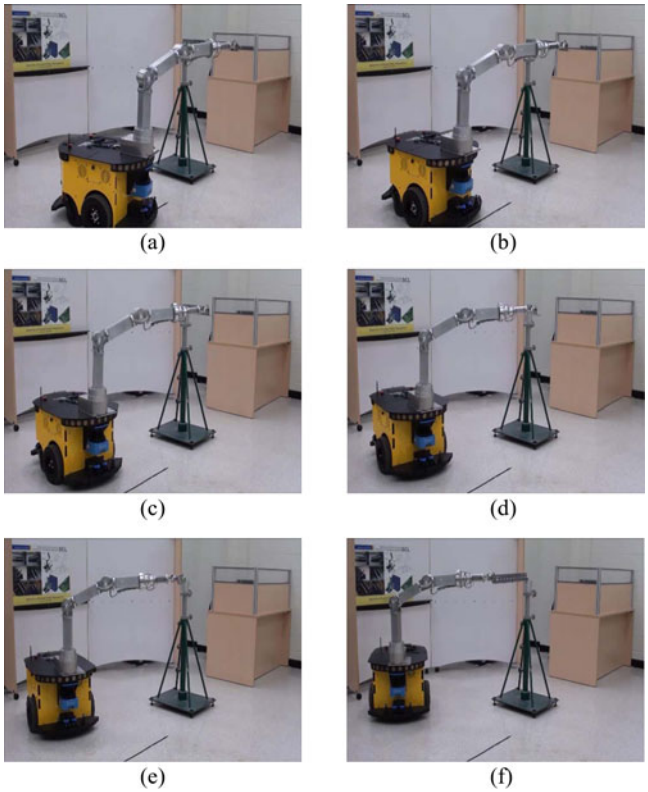

Fig. 10. Pictures of the mobile MRR pulling door open. Picture (a) shows the start position; (b) the mobile base started following the desired path with MRR joints 1, 4 and 5 are working in passive mode; (c), (d), and (e) the yaw angle of the DAUJ has changed (see Fig. 12 for the yaw angle and the corresponding motion time); (f) door is completely open, 90°.

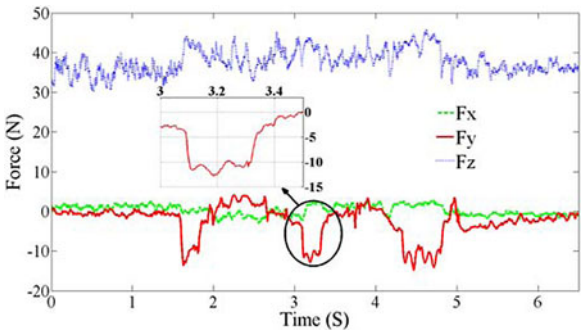

Fig. 11. Force measurements at the MRR end-effector.

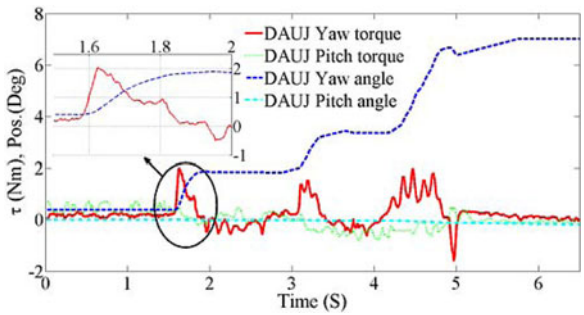

Fig. 12. DAUJ pitch and yaw positions and torques.

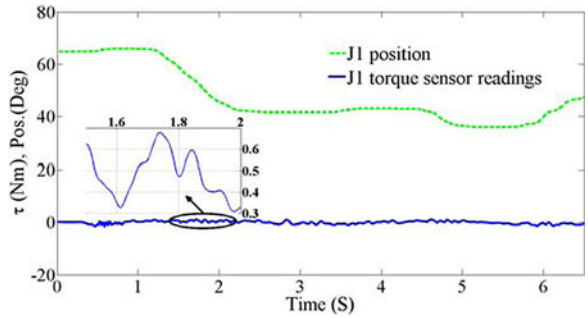

Fig. 13. Torque sensor readings and joint angle of the MRR joint 1.

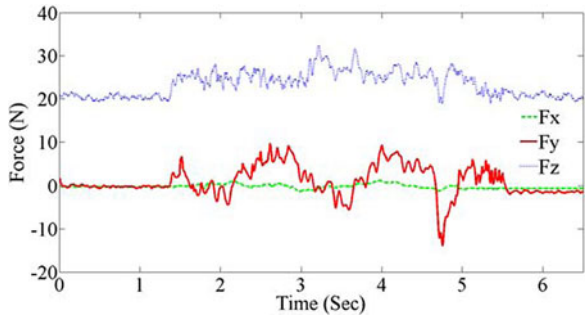

Fig. 14. End-effector forces with 2° heading angle error.

the door-opening process. The torque measurements at the wrist were less than 2.3 N·m. It is worth noting that the DAUJ has a threshold of around 2 N·m before it starts moving when working in passive mode. This is partially due to the uncompensated part of the joint friction. This threshold is necessary to prevent DAUJ motion in absence of external forces as a result of the gripper weight and it has been selected experimentally by trial and error. This means that the measured internal forces are less than 0.3 N·m. In comparison to the previously proposed door-opening methods, these internal forces are of similar magnitude to those achieved when using complicated compliant control algorithms. Experiments also showed that the proposed method is robust to the accumulated positioning errors of the mobile base. This was confirmed by repeating the experiment with different initial heading angles of the mobile base to change its trajectory while making sure it was still within the allowed margin. The mobile MRR could open the door with measured internal forces that are still of comparable magnitude to the case in which no heading error is introduced. For example, the torque measurements at the wrist reached a maximum of 3 N·m when offsetting the mobile base initial heading angle by 2°. The results of the door-opening experiment when mobile base heading angle error is introduced are shown in Fig. 14–16. The torque measurements at the wrist, as shown in Fig. 15, are similar to those of the previous experiment. During the experiments, it was noticed that there was minor relative motion between the robot end-effector and the door knob. This minor relative motion did not affect the door-opening performance, as the free joints are passively controlled by the coupling forces between the MRR and the door, which do not depend on the contact point.

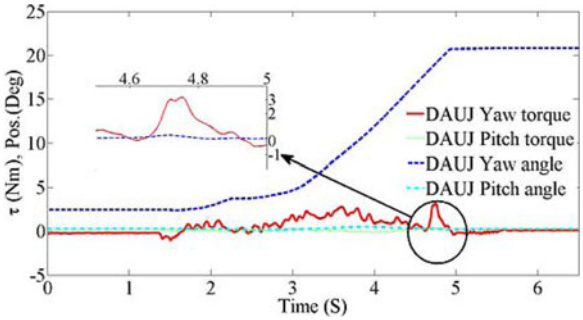

Fig. 15. DAUJ angles and torques with 2° heading angle error.

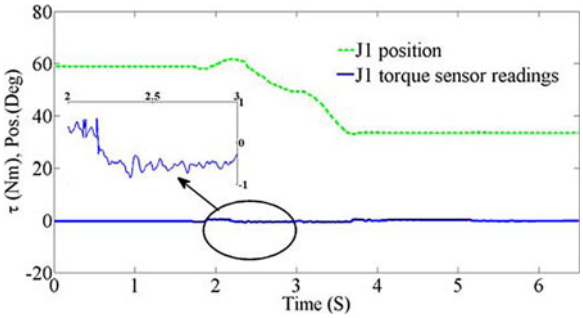

Fig. 16. Joint 1 angle and torque sensor readings with 2° heading angle error.

VII. Conclusion

In this paper, we have presented a novel door-opening method with experimental demonstration using a mobile MRR. By switching between active and passive working modes of the MRR joint modules, the occurrence of large internal forces was prevented. The presented method solves a major problem of door-opening without using complicated control algorithms or any special mechanical design, and it can be implemented on any other robot that has joints capable of working in both active and passive modes. The use of the multiple working modes of the MRR joint modules will be further investigated in some other mobile manipulator applications. The next goal of this paper is to realize autonomous door localization and door knob grasping based on a stereo vision system. Work will be also directed toward pushing doors open and opening spring-loaded doors.

References

[1] S. Katsura, Y. Matsumoto, and K. Ohnishi, "Modeling of force sensing and validation of disturbance observer for force control," *IEEE Trans. Ind. Electron.*, vol. 54, no. 1, pp. 530–538, Feb. 2007.

[2] S. Kobayashi, Y. Kobayashi, Y. Yamamoto, T. Watanabe, Y. Ohtsubo, T. Inoue, M. Yasuda, and Y. Takamori, "Development of a door opening system on rescue robot for search' UMRS-2007'," in *Proc. SICE Annu. Conf.*, Tokyo, Japan, Aug. 20–22, 2008, pp. 2062–2065.

[3] P. Lawrence and S. Erik, "Door breaching robotic manipulator," presented at the SPIE Defense Security Conf., Orlando, FL, Mar. 2008.

[4] K. Nagatani and S. Yuta, "Designing a behavior to open a door and to pass through a door-way using a mobile robot equipped with a manipulator," in *Proc. IEEE/RSJ Int. Conf. Intell. Robots Syst.*, Munich, Germany, Sep. 12–16, 1994, pp. 847–853.

[5] K. Nagatani and S. Yuta, "An experiment on opening-door-behavior by an autonomous mobile robot with a manipulator," in *Proc. IEEE/RSJ Int. Conf. Intell. Robots Syst.*, Pittsburgh, PA, Aug. 5–9, 1995, pp. 45–50.

[6] K. Nagatani and S. Yuta, "Designing strategy and implementation of mobile manipulator control system for opening door," in *Proc. IEEE Int. Conf. Robot. Autom.*, Minneapolis, MN, Apr. 22–28, 1996, pp. 2828–2834.

[7] G. Niemeyer and J. J. E. Slotine, "A simple strategy for opening an unknown door," in *Proc. IEEE Int. Conf. Robot. Autom.*, Albuquerque, NM, Apr. 20–25, 1997, pp. 1448–1453.

[8] L. Petersson, D. Austin, and D. Kragic, "High-level control of a mobile manipulator for door opening," in *Proc. IEEE/RSJ Int. Conf. Intell. Robots Syst.*, Takamatsu, Japan, Oct. 31–Nov. 5, 2000, pp. 2333–2338.

[9] D. Kragic, L. Petersson, and H. Christenseni, "Visually guided manipulation tasks," *Robot. Auton. Syst.*, vol. 40, no. 2–3, pp. 193–203, Aug. 2002.

[10] B. J. W. Waarsing, M. Nuttin, and H. Van Brussel, "Behaviour-based mobile manipulation: The opening of a door," in *Proc. 1st Int. Workshop Adv. Serv. Robot.*, Bardolino, Italy, Mar. 13–15, 2003, pp. 170–175.

[11] W. Chung, C. Rhee, Y. Shim, H. Lee, and S. Park, "Door-Opening control of a service robot using the multifingered robot hand," *IEEE Trans. Ind. Electron.*, vol. 56, no. 10, pp. 3975–3984, Oct. 2009.

[12] D. Kim, J. Kang, C. Hwang, and K. Park, "Mobile robot for door opening in a house," in *Knowledge-Based Intelligent Information and Engineering Systems*. vol. LNAI-3215. New York: Springer-Verlag, Oct. 2004, pp. 596–602.

[13] R. Brooks, L. Aryananda, A. Edsinger, P. Fitzpatrick, C. Kemp, U. M. O'Reilly, E. Torres-Jara, P. Varshavskaya, and J. Weber, "Sensing and manipulating built-for-human environments," *Int. J. Humanoid Robot.*, vol. 1, no. 1, pp. 1–28, 2004.

[14] E. Klingbeil, A. Saxena, and A. Ng, "Learning to open new doors," presented at the AAAI 17th Annu. Robot Workshop Exhib., Chicago, IL, Jul. 13–17, 2008.

[15] G. Liu, X. He, J. Yuan, S. Abdul, and A. A. Goldenberg, "Development of modular and reconfigurable robot with multiple working modes," in *Proc. IEEE Int. Conf. Robot. Autom.*, Pasadena, CA, May 19–23, 2008, pp. 3502–3507.

[16] W. Li and J. J. E. Slotine, "A unified approach to compliant motion control," in *Proc. Amer. Control Conf.*, Pittsburgh, PA, Jun. 21–23, 1989, pp. 1944–1949.

[17] A. Jain and C. C. Kemp, "Pulling open doors and drawers: Coordinating an omni-directional base and a compliant arm with Equilibrium Point control," in *Proc. IEEE Int. Conf. Robot. Autom.*, Anchorage, AK, May 3–7, 2010, pp. 1807–1814.

[18] S. Ahmad and G. Liu, "A door opening method by modular re-configurable robot with joints working on passive and active modes," in *Proc. IEEE Int. Conf. Robot. Autom.*, Anchorage, AK, May 3–8, 2010, pp. 1480–1485.

[19] S. Ryew and H. Choi, "Double active universal joint (DAUJ): Robotic joint mechanism for human-like motions," *IEEE Trans. Robot. Autom.*, vol. 17, no. 3, pp. 290–300, Jun. 2001.

[20] G. Strang, *Introduction to Applied Mathematics*. Wellesley, MA: Wellesley-Cambridge Press, 1986.

[21] W. Imran and F. Reza, "Trajectory and temporal planning of a wheeled mobile robot on an uneven surface," *Robotica*, vol. 27, pp. 481–498, 2009.

[22] B. Armstrong-Helouvry, P. Dupont, and C. Canudas De Wit, "Survey of models, analysis tools and compensation methods for the control of machines with friction," *Automatica*, vol. 30, pp. 1083–1138, Jul. 1994.

[23] M. Wang, S. Ma, B. Li, and Y. Wang, "Reconfiguration of a group of wheel-manipulator robots based on MSV and CSM," *IEEE/ASME Trans. Mechatronics*, vol. 14, no. 2, pp. 229–239, Apr. 2009.

[24] G. Liu, Y. Liu, and A. A. Goldenberg, "Design, Analysis, and control of a spring-assisted modular and reconfigurable robot," *IEEE/ASME Trans. Mechatronics*, vol. 16, no. 4, pp. 695–706, Aug. 2011.

[25] G. Liu, S. Abdul, and A. A. Goldenberg, "Distributed control of modular and reconfigurable robot with torque sensing," *Robotica*, vol. 26, pp. 75–84, 2008.

[26] J. Imura, T. Sugie, Y. Yokokohji, and T. Yoshikawa, "Robust control of robot manipulators based on joint torque sensor information," in *Proc. Workshop Intell. Robots Syst.*, Osaka, Japan, Nov. 3–5, 1991, pp. 344–349.

[27] G. Liu, A. A. Goldenberg, and Y. Zhang, "Precise slow motion control of a direct-drive robot arm with velocity estimation and friction compensation," *Mechatronics*, vol. 14, no. 7, pp. 821–834, Sep. 2004.

[28] G. Liu, A. A. Goldenberg, and Y. Zhang, "Uncertainty decomposition based robust control of robot manipulators," *IEEE Trans. Control Syst. Technol*, vol. 4, no. 4, pp. 384–393, Jul. 1996.

[29] G. Liu, Decomposition-based friction compensation of mechanical systems, *Mechatronics*, vol. 12, no. 5, pp. 755–769, 2002.

Saleh Ahmad received the B.Sc. degree in electronics engineering from Sebha University, Sebha, Libya, and the M.Sc. degree in control engineering from Lakehead University, Thunder Bay, ON, Canada, in 1999 and 2008, respectively. He is currently working toward the Ph.D. degree in the Department of Aerospace Engineering, Ryerson University, Toronto, ON.

His current research interests include mobile manipulation, multiple working modes control design for modular and reconfigurable robots, as well as the design and development of fault detection, and isolation schemes for mobile modular and reconfigurable robots.

Hongwei Zhang received the B.Sc. degree from the University of Science and Technology of China, Hefei, China, in 1990, and the M.E. degree from Tongji University, Shanghai, China, in 1993. In 2008, he joined the Department of Aerospace Engineering, Ryerson University, Toronto, ON, Canada as a Ph.D. student.

His research interests are in the areas of multiple working modes control design for modular and reconfigurable robots, in particular, the control design and implementation of novel passive mode algorithms. His research also focuses on the precise modeling of harmonic drive transmission taking into account the hysteresis properties, nonlinear friction dissipation, and kinematic error.

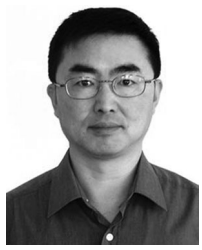

Guangjun Liu (M'99–SM'08) received the B.E. degree from the University of Science and Technology of China, Hefei, China, in 1984, the M.E. degree from the Chinese Academy of Sciences, Shenyang Institute of Automation, Shenyang, China, in 1987, and the Ph.D. degree from the University of Toronto, Toronto, ON, Canada, in 1996.

From 1997 to 1999, he was a Systems Engineer and a Design Lead for Honeywell Aerospace Canada, where he was involved in the Boeing X-32 program. In 1996, he was a Postdoctoral Fellow at the Massachusetts Institute of Technology, Cambridge. He is currently a Professor and Canada Research Chair in Control Systems and Robotics in the Department of Aerospace Engineering, Ryerson University, Toronto. He has authored or coauthored more than 150 papers in international journals and conference proceedings. His current research interests include control systems and robotics, particularly in modular and reconfigurable robots, mobile manipulators, and aircraft systems.

Dr. Liu is a Technical Editor of the IEEE/ASME TRANSACTIONS ON MECHATRONICS and a Licensed Member of the Professional Engineers of Ontario, Canada.